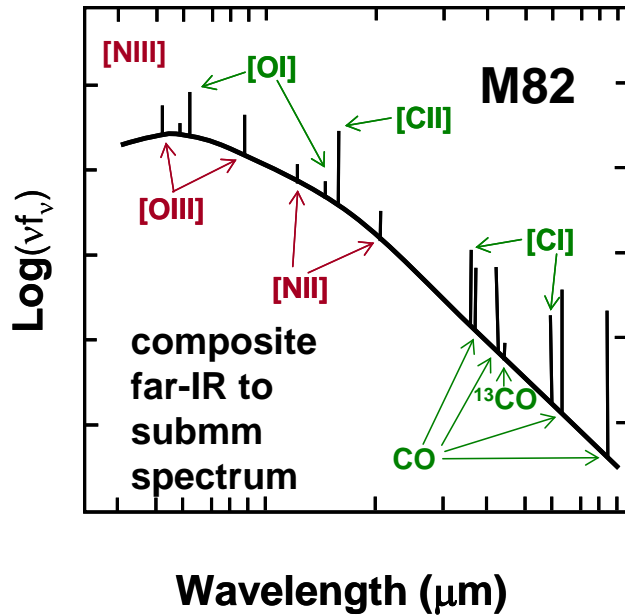
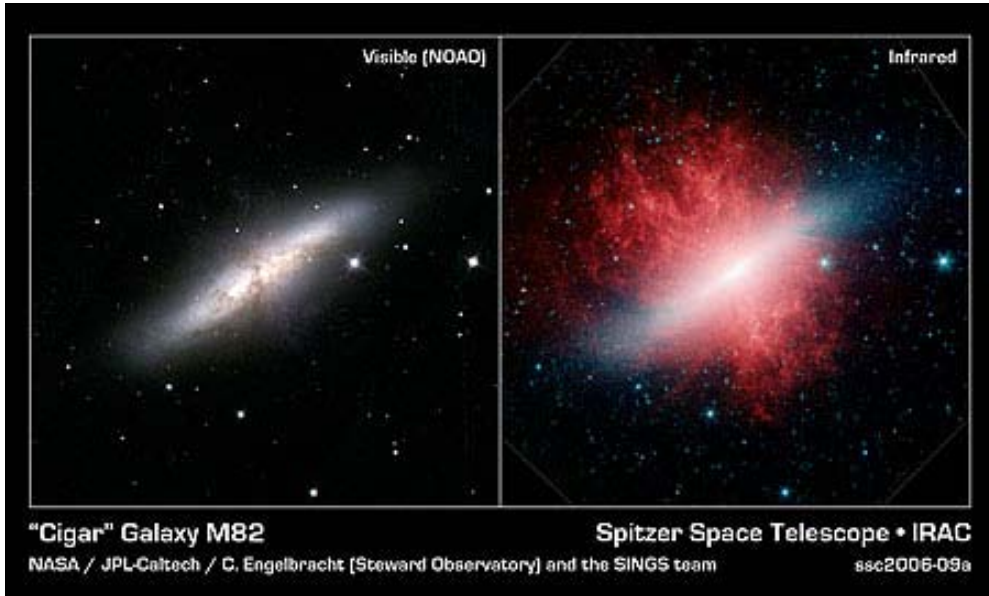


Star Formation Through Cosmic Time: From Local Galaxies to the Early Universe*

Gordon J. Stacey (gjs12@cornell.edu)
Department of Astronomy, Cornell University, Ithaca, NY
607-255-5900

Frank Bertoldi (U. Bonn), A.W. Blain (Caltech), C.M. Bradford (JPL), Riccardo Giovanelli (Cornell), Jason Glenn (Colorado), Paul Goldsmith (JPL), Sunil Golwala (Caltech), Thomas Nikola (Cornell), and Jonas Zmuidzinas (Caltech)



*A whitepaper submitted on 2/15/09 in response to the call from the Astro2010 panel

Motivation

The star formation rate per unit co-moving volume in the Universe peaked when the Universe was only 15-45% of its present age ($1 < z < 3$) at values 30 times the present rate. To understand the processes which produced this strong evolution of star formation over cosmic time, it is important to study nearby, spatially resolved systems so that one can relate the astrophysical probes and lessons learned to the high redshift, unresolved systems. As in the present epoch, it seems that many, if not most of the star-forming galaxies in the early Universe are dusty, often extremely dusty so that it is impossible to directly view the star-formation regions themselves at these times with rest-frame optical/UV probes only. The overwhelming presence of dust also ensures that most of the energy of these sources – be it released through nuclear or gravitational process – emerges in the rest frame far-IR bands.

Resolved images of nearby galaxies in these bands will reveal the interplay between the star formation process and the natal ISM in these systems, providing the templates necessary to understand the line emission from distant, unresolved galaxies. Of particular interest is resolving the most active regions in nearby normal and starburst galaxies, as it is these regions that will provide the best templates for distant, LIRG and ULIRG-class galaxies which appear to be responsible for the bulk of the cosmic far-IR background. Multi-wavelength studies will, for example, trace the process of gas compression in spiral density waves, the formation of stars in molecular cloud cores, and the disruption of the parent clouds by these newly formed stars. What are the relationships between the age (abundances) of the ISM, degree of star formation activity, galactic morphology, and environment? Do different galaxies have different IMFs? What triggers galaxy wide bursts of star formation? Do starbursts “burn themselves out” by consuming all the available fuel and/or disrupting the natal environment through stellar winds?

Fortunately, the far-IR and submillimeter spectral regime provides a wide variety of spectral probes of both ambient radiation fields and the physical properties of the gas. Most of these lines lie only a few hundred K above the ground state, have modest critical densities, and the emitted radiation is nearly always optically thin. Therefore, these lines provide important, if not the dominant coolants for the most important phases of the interstellar medium including the warm ionized medium (WIM), the cold neutral medium (CNM), the warm neutral medium (WNM), and the photodissociated surfaces and shielded interiors of molecular clouds. They also provide important, extinction free probes of both the physical conditions of the gas (density, temperature, dynamics), and the properties of the exciting radiation fields (intensity and hardness).

1. Far-IR/Submm Lines

The most important far-IR/submm lines include the 10 fine structure lines from abundant species ($C^0, C^+, N^+, N^{++}, O^0, O^{++}$) plus the mid-J ($J \sim 4-3$ to $13-12$) rotational transitions of CO. These lines are primarily tracers of star formation (Figure 2), and are very bright in star forming galaxies, often summing to more than 1% of the total luminosity of the galaxy (Figure 1). In addition to the far-IR lines, there are important tracers in the 12 to 40 μm spectral regime that are well described in the Armus et al. white paper. The importance of the far-IR/submm dust continuum – which often transfers the bulk of the luminosity, is explicated in the Blain et al. white paper.

Cover (Fig.1) Optical (above left), and Spitzer (above right) views of the starburst galaxy M82. (left) Composite spectrum of M82 including observed far-IR and submm lines (Colbert et al. 1999, Stutzki et al. 1997, Ward et al. 2003, Petuchowski et al. 1994)

1.1. Ionized Gas Lines.

The [NII], [NIII], and [OIII] lines arise from ionized gas regions, and since they arise from levels only a few hundred K above the ground, are very insensitive to the gas temperature. The [NII] pair is a density probe for low density HII regions, while the [NII]/[NIII] line ratios are excellent probes of the hardness of the impinging radiation fields –

a flipping point from strong emission in the [NII] lines to strong emission in the [NIII] line occurs for spectral types earlier than \sim O8. It takes

roughly the same UV photon energy to form O^{++} as it does to form N^{++} , so that the [NIII] and [OIII] lines arise from similar ionization state HII regions and the trio of lines form a good probe of the N/O abundance ratio (Lester et al. 1987). Enhanced N/O ratios are indicators of past star formation, so that this ratio directly relates to the evolution of the ISM. The [OIII] line pair constrains the gas density for the higher ionization state HII regions around early type stars. The combination of ionized gas lines therefore track the locations and spectral types of ionizing stars, so that they can yield the present day high mass cutoff for stars as a function of galactic radius, and in relation to spiral arms or bar potentials.

The [CII] line also arises from ionized gas, but is strongest in the neutral ISM. The [NII] 205 μ m line has the same critical density as the [CII] line in ionized gas, so that the line ratio yields the fraction of the observed [CII] emission that arises from HII regions (Oberst et al. 2006). It is important to account for and remove the [CII] flux arising in HII regions when modeling the cooling of the neutral ISM.

Interior to the [CII] and [OI] emitting “surface” of PDRs, lies first a transition to a thin neutral carbon region, then a region of warm, dense molecular gas where C is tied up predominantly in CO. These regions emit strongly in the [CI] and mid-J CO lines, and their line intensities are a measure of the physical conditions of the gas. The [CI] lines have modest

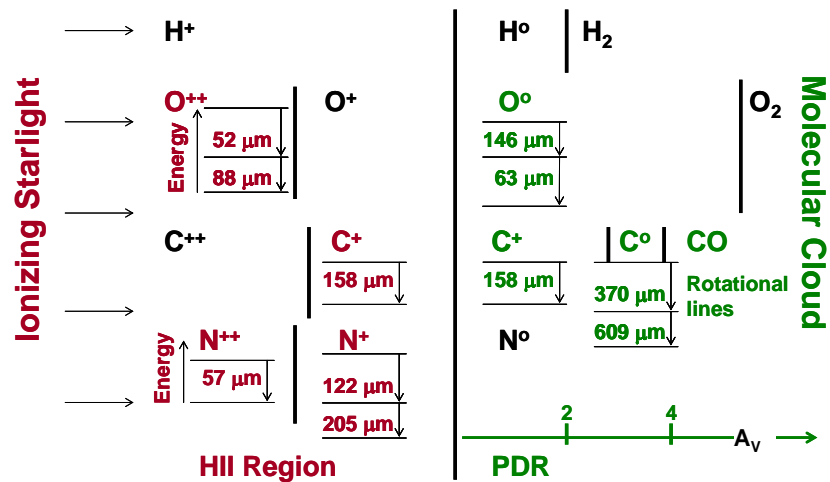


Fig. 2 Sketch of a molecular cloud exposed to the ionizing radiation from an O6 star. Starlight enters from the left forming an HII layer which emits far-IR [OIII], [NIII], [NII] and [CII] line radiation. Deeper into the cloud the gas is neutral and now emits in the [CII], [OI], [CI] and CO lines in the far-IR/submm bands

critical densities, and are usually optically thin so that their ratio yields the gas temperature, and their absolute intensities yields gas column density. The mid-J CO lines have much larger excitation requirements so they track warmer, denser gas.

The CO molecule is typically the dominant coolant for molecular gas. The run of line intensity with J constrains the gas temperature, density and mass. The ^{12}CO lines are often optically thick, so it is important to measure ^{13}CO lines as well. CO studies are quite important, as it is the molecular gas reservoir that constrains future episodes of star formation. The low-J line CO and isotopic lines cool the cold cores of molecular clouds, and trace their mass. The mid-J line emission signals the presence of PDRs associated with newly formed OB stars, while the high J lines trace molecular shocks from outflows, turbulence or cloud-cloud collisions.

Of particular interest are the [CI] 370 μm line and the CO(7 \rightarrow 6) line pair. Since they lie only 2.7 GHz (1000 km/sec) apart, they are easily observed simultaneously in one extragalactic spectrum yielding excellent relative calibration and “perfect” spatial registration. The line ratio is very density sensitive, and can be used to rapidly pick out heavily extinguished star formation regions via their enhanced CO(7 \rightarrow 6) line emission (Figure 3).

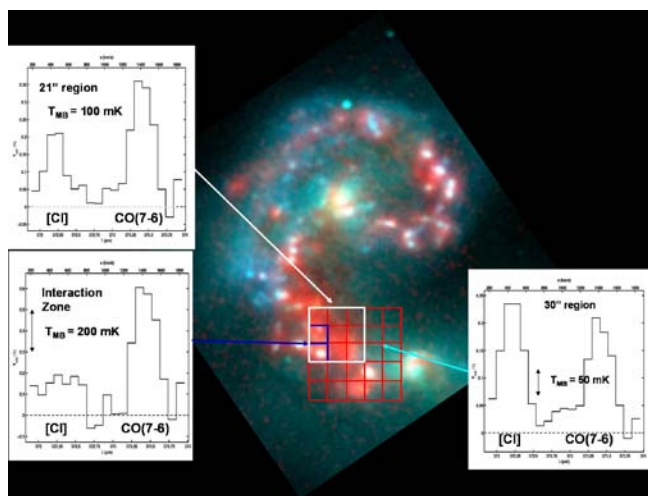


Fig. 3 Simultaneous mapping of CO(7 \rightarrow 6) and [CI] 370 μm line emission from the Antennae system obtained using the SPIFI imaging Fabry-Perot on the JCMT (Isaak et al. 2009). The squares indicate the positions of the various pixels in SPIFI’s imaging array. Averaged over a 16 pixel (28” \times 28”) footprint the [CI] line is somewhat brighter than the CO line (right-most spectrum). As one zooms into a 21” \times 21” region, the CO line becomes brighter than the [CI] line (top-left spectrum). At the position of the starburst (lower-left spectrum), the CO line is greatly enhanced, reflecting the higher gas densities there.

2. Applications

2.1. Star Formation in Spiral Galaxies It is important to map a variety of nearby galaxies and resolve the different regimes in their far-IR and submm spectral lines. Several nearby systems are planned for mapping with instrumentation on Herschel. To date, the best example of a resolved system, mapped in the bright far-IR fine structure lines is M83, a bright, nearby barred Sc galaxy presented to us nearly face on. M83 was mapped in the [OI], [NII] 122 μm , [OIII], [NIII], and [CII] lines with the ISO LWS (70” beam, Figure 4). All lines are detectable over the entire galaxy, and the sum total line luminosity is about 1% of the total far-IR continuum. Half of this line emission comes out in the [CII] line alone. Given the relative ratio of the [CII] to [NII] 122 μm lines, and assuming the low density limit, about 35% of the [CII] emission arises from the ionized gas. The [CII]/[OI]/[NII] line ratios are roughly constant across the spiral arms suggesting the mix in the ISM (dense PDRs, atomic clouds, diffuse ionized gas) is constant across the arm and interarm. Most of the [CII] and [OI] arise from higher density PDRs on the surfaces of molecular clouds with typical densities $\sim 3000 \text{ cm}^{-3}$, exposed to far-UV fields $G \sim 3000$ times the local (Habing) interstellar radiation field.

The spiral arm/inter-arm contrast is highest for the [OIII] 88 μm line, and at the bar-spiral arm interfaces indicating the presence of early O stars therein. Furthermore, the [OI], [OIII], and [CII] lines are all strongly enhanced at the bar-spiral arm interfaces, and best fit by intense HII regions dominated by O6 stars exposing the local neutral medium to very intense far-UV radiation fields similar to those at the Orion interface region 0.2 pc from an O5 star! This region is strong in the CO line emission as well. Presumably the intense starformation there is triggered by orbit crowding collisions of molecular clouds.

It is very important to observe these lines at the highest possible spatial resolution – resolution sufficient to pick out individual star formation complexes, and compare the line emission to the [NII] 205 μm , [CI] and mid-J CO line emission at similar or better resolution. In this way, important tracers, and coolants of all of the major phases of the ISM can be analyzed together revealing the processes of star formation, and its interplay with the natal ISM. Can we trace the compression of gas ready for the subsequent “ignition” of the next generation of stars?



Figure 4. (left) ISO LWS map of M83 ($d=4.5$ Mpc) in the [CII] line (contours, 70'' beam) superposed on an optical image. (middle) IRAC 8 μm (2'' beam) and (right) MIPS 24 μm (6'' beam) continuum image of M81 ($d=3.5$ Mpc). Next generation far-IR/submm generation will enable imaging of nearby galaxies in the *far-IR/submm lines* at spatial resolutions comparable to the IRAC and MIPS images (e.g. [OIII] (52 μm) $\sim 3''$ with 3.5 m SPICA telescope, [NII] 205 μm and [CI] 370 μm ~ 1.7 and 3'' respectively with 25 m CCAT telescope.)

2.2. Molecular Gas in Starburst Galaxies. Mid-J CO line emission has been detected from more than two dozen nearby infrared bright galaxies showing the preponderance of warm dense gas. The brightest extragalactic source is the starburst nucleus of NGC 253 which has been extensively mapped in CO(4-3), (6-5), and (7-6), and most recently been detected in $^{13}\text{CO}(6-5)$ (Hailey-Dunsheath et al. 2008) with intriguing results. The run of ^{12}CO , and ^{13}CO line emission with J is consistent with *half of the molecular gas* residing in a single warm ($T \sim 120$ K), dense ($n \sim 4.5 \times 10^4 \text{ cm}^{-3}$) component. This component also can account for the observed H_2 rotational line emission. Since the mass of this warm molecular gas is 10 to 30 times larger than that in PDRs as traced by their [CII] and [OI] line emission, it appears unlikely that the gas is heated by far-UV photons in a PDR scenario. Instead, it appears likely that the gas is heated either by the greatly enhanced cosmic ray flux (~ 800 times the Milky Way value) in the starburst nucleus, or through dissipation of turbulent energy within the clouds. Both sources would provide a natural mechanism for heating the entire volume of molecular gas, and presuming they have their origins in the starburst, the added heat at the cloud cores from cosmic rays and/or dissipation of turbulent energy will inhibit cloud collapse, so that the starburst in NGC 253 is self-limiting.

3. Distant Galaxies

The observations outlined above are necessary to properly understand the star formation process on galactic scales in the local Universe, and they are of fundamental importance as templates through which one can interpret observations of these lines from unresolved star forming galaxies in the distant Universe.

Dust and metals are prominent in the early Universe, and the large mm-arrays have enabled an industry of detecting and mapping the cooling mid-J CO line emission from distant ($z > 2$) galaxies. This pioneering work discovered the enormous reservoirs of molecular fuel in these systems necessary to spawn their tremendous star formation rates (Tacconi et al. 2006). This work will be greatly advanced by the enormous collecting area of ALMA. However, single dish observatories, such as CCAT enable complementary science. For instance, obtaining the redshifts for the dusty, very optically faint submillimeter galaxies, have

proven exceedingly challenging (Chapman et al. 2005). A suitably broadband spectrometer can detect several CO lines within one spectrum, not only characterizing the molecular ISM, but delivering an unambiguous redshift ($\text{CO line spacing} = 115 \text{ GHz}/(1+z)$) of the system. For example, the direct detection spectrometer, Z-Spec recently detected four mid-J CO lines from the luminous, lensed Cloverleaf system in a single spectrum (Figure 5). The line spacing reflects the redshift, the line intensity ratios constrain the physical conditions of the gas, and the broad bandwidth enables searches for other lines. *Water lines* are detected for the first time in the system.

Detecting the $158 \mu\text{m}$ [CII] line from distant galaxies is important, since it is a dominant coolant, and the [CII] to far-IR continuum luminosity ratio is a measure of the strength of the ambient interstellar radiation field. Clearly, however, there is enhanced scientific pay-off when one detects and resolves galaxies in a variety of tracers. Here we present a recent detection of the [CII] line from a super-starburst galaxy at $z = 1.3249$, combined with interferometric imaging of the CO(3-2) and (2-1) lines and PDR modeling as an example of the science one can pursue.

Redshifted [CII] emission has only been reported from a very small number of sources, including the detection of weak line emission from a two quasars, one at $z = 6.42$ (Maiolino et al. 2005). Recently, however, strong [CII] line emission is reported from the “super-starburst” galaxy MIPS J142824.0 +352619 at $z = 1.3249$ using a direct detection grating spectrometer, ZEUS, on the CSO (Hailey-Dunsheath et al. 2009). MIPS J142824 is a compact, red object discovered in the MIPS deep Bootes field survey, with an extreme rest-frame far-IR luminosity

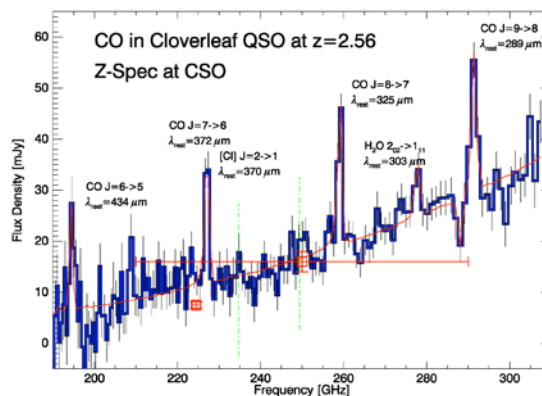


Fig. 5 Multi-line spectrum of the $z=2.56$ Cloverleaf Quasar. Visible are 4 mid-J lines of CO, the [CI] $370 \mu\text{m}$ line (mixed with CO(7-6)), and a water line (Bradford et al. 2009)

MIPS J142824.0+352619

[CII] at $z = 1.3249$

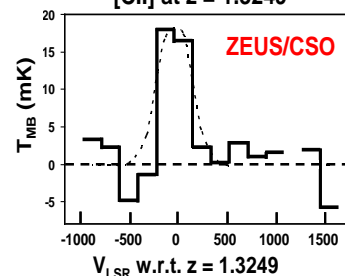


Fig. 6. [CII] line from the hyperluminous galaxy MIPS J142824 (Hailey-Dunsheath et al. 2009)

($L_{\text{far-IR}} \sim 3.2 \times 10^{13} L_{\odot}$) – although it may be lensed by a factor of eight. The far-IR to submm SED and IR/radio continuum luminosity ratio is consistent with MIPS J142824 being a super starburst galaxy forming stars at a rate near $3000 M_{\odot}$ per year. MIPS J142824 has also been imaged in CO(2-1) and CO(3-2). The source fluxes and distribution indicate that $10^{11} M_{\odot}$ of molecular gas is concentrated in a region less than 15 kpc across (Iono et al. 2006).

The [CII] line is strongly detected with a [CII]/far-IR continuum luminosity ratio similar to that found in nearby starburst galaxies. This high ratio indicates far-UV fields $G \sim 2000$. Since the far-IR intensity relates to the far-UV intensity, comparing the observed far-IR intensity to the derived G yields the beam filling factor, hence source size, which is large, ~ 3 kpc. The CO line ratios are density sensitive, so that combining the [CII], CO, and far-IR continuum with PDR models (“Web Infrared Tool Shed”) yields a unique solution: $G \sim 2000$, $n \sim 3 \times 10^4 \text{ cm}^{-3}$. The conclusion is that MIPS J142824 is undergoing a galaxy-wide starburst supporting the contention that hyper-luminous systems may be giant elliptical galaxies in formation.

4. Facilities

4.1. SOFIA/Herschel/SPICA The SOFIA and Herschel platforms with their 2.5 and 3.5 m apertures respectively provide the best near term facilities from which to observe spectral lines that are unavailable to even at the best ground based sites. These include the [OIII] (52 and 88 μm), [OI] 63 and 146 μm), [CII] (158 μm), and [NII] (122 μm). While the apertures of SOFIA and Herschel are modest, these are the shorter wavelength far-IR and submm lines so that spatial resolutions of the order 5” ([NII] 52 μm with SOFIA) to 12” ([CII] with Herschel) are possible, enabling a separation of arm/interarm regions and star formation complexes in nearby systems (at 5 Mpc, 5” \Leftrightarrow 120 pc), so that the formidable diagnostic power of these lines can be brought to bear. Herschel has the advantage of somewhat larger aperture, and since it is above the atmosphere, it is more sensitive than SOFIA in the 75 to 180 μm regime. However, SOFIA can benefit from instrument upgrades. For instance, an optimized image slicing spectrometer on SOFIA, equipped with a state-of-the-art bolometer array, rather than photoconductors, would have sensitivity within a factor of 2 of PACS/Herschel in the 75-180 μm regime, and somewhat better at both shorter and longer wavelengths. Furthermore, SOFIA can take advantage of increases in array format (pixel count) providing an advantage in mapping speed. On the other hand, being in space, Herschel is never subject to interference from telluric lines. While not typically a problem at aircraft altitudes, it is a problem for SOFIA for the astrophysically important [OI] 63 μm line, that is obscured at redshifts between 500 km/sec and 1600 km/sec.

With a bolometer equipped grating spectrometer, SOFIA is capable of detecting the [CII] line from $z = 0$ to 1 with uniquely high sensitivity in the $z = 0.25$ to 1 range, the [NII] 122 μm and 205 μm lines from $z = 0.65$ to 1.3 and 0 to 0.65 respectively. Herschel can provide complementary observations of the [OI] 63 μm and [OIII] lines. These observations provide important links between the nearby galaxies and the more distant galaxies explored with the large aperture ground based facilities such as CCAT and ALMA (below).

In the somewhat longer term, the 3.5 m cryogenic (4.5 K) aperture of the Japanese SPICA mission provides an exquisitely sensitive platform from which one can observe the far-IR lines. The US community has put forth a concept for a direct detection spectrometer (BLISS) covering the 40 to 600 μm regime that promises to be **2 to 3 orders of magnitude** more sensitive than either Herschel or SOFIA. This translates into 4-6 orders of magnitude increase in mapping

speed, and, with BLISS / SPICA observations of the important lines are enabled for exceedingly faint systems throughout the era of peak activity in galaxies to redshifts beyond ~ 5 .

4.2. CCAT. The nearby galaxies make excellent targets for the planned 25 meter Cornell Caltech Atacama Telescope (CCAT). Located near the summit of Cerro Chajnantor, high above the ALMA site, the precipitable water vapor content is sufficiently small so that observations in the short submm bands (350 and 450 μm) will be routine, and even observations in the 200 μm window will be common. Therefore, CCAT can deliver spectroscopic images of galaxies in the [NII] 205 μm , [CI] 370 and 609 μm , and mid-J CO (e.g. 4-3, 6-5, 7-6), and ^{13}CO (6-5 & 8-7) rotational lines at spatial resolutions as fine as $2''$, which corresponds to 50 pc at the distance of M83 (4.5 Mpc). In the nuclei of some galaxies (e.g. ULIRGs) one might expect to detect CO emission up to $J = 13-12$ (200 μm) arising from nuclear clouds highly excited by starbursts, or even CO emission from AGN excited molecular tori.

The large aperture and superb site also enables observations of distant galaxies. The [CII] line is readily detectable at redshifts from 0.25 to beyond 5 with telluric windows open over $>50\%$ of this range (Figure 7). Galaxies as faint as $L_{\text{far-IR}} \sim 3 \times 10^{11} L_{\odot}$ are readily detectable beyond redshift 5. The other fine structure lines are also detectable with some telluric gaps, for instance the [NII] 122 and 205 μm lines at redshifts ~ 0.7 & 1.6 to 3, and 0 & 0.5 to 3.9 respectively, the [OIII] 88 μm at $z \sim 1.3$ & 2.6 to 4.5, and the [OI] 63 μm line at $z \sim 2.3$ & 4 to 5. With a broad-band, optimized spectrograph several of these lines can be detected simultaneously. A multi-object “fiber” fed spectrometer enables spectroscopy for tens of objects within the large ($20'$) field of view of the CCAT dish, multiplexing the science. The numbers of these bright objects at present are modest, but the powerful continuum surveys of CCAT will reveal many thousands of candidate sources (see Blain et al. white paper for details).

4.3. ALMA ALMA will provide unchallenged spatial resolution at high sensitivity in the mid-J CO and [CI] lines. Subarcsecond resolution enables tracing the neutral gas clouds at the subpc scales for many galaxies in the local Universe. For example, in the [CI] 806 GHz line, ALMA can resolve features as small as 0.007 arcsec, or 0.15 pc at the distance of M83. The field of view, however, is somewhat limited ($\sim 7''$ at 350 μm) so that extensive, and challenging mosaicing of fields are required for large scale ($5'$) maps. Therefore, CCAT and ALMA together are a powerful duo. CCAT, with large format imaging spectrometers can map entire galaxies such as M83 and ALMA can “zoom in” to study regions of particular interest.

References. Blain et al. 2002, Bradford et al. 2009, Chapman et al. 2005, Colbert et al. 1999, Hailey-Dunsheath et al. 2008, Iono et al. 2006, Isaak et al. 2009, Lester et al. 1987, Maiolino et al. 2005, Oberst et al. 2006, Petuchowski et al. 1994, Stacey et al. 1985, Stutzki et al. 1997, Tacconi et al. 2006, Ward et al. 2003, Wright et al. 1991.

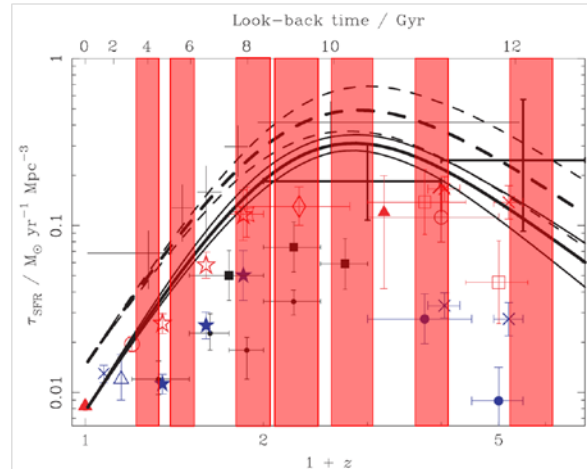


Figure 7. Redshifts for [CII] observations available in the short submm telluric windows at the Chajnantor site for CCAT superposed on estimates for the star formation per unit comoving volume as a function of $1+z$ (Blain et al. 2002, Phys. Rep., 369, 111)